International Journal of Modern Physics E

Investigation of the low-energy K^- Hadronic Interactions with Light Nuclei by AMADEUS

Magdalena Skurzok[1,2,*], Massimiliano Bazzi[2], Mario Bragadireanu[3], Damir Bosnar[4], Michael Cargnelli[5], Alberto Clozza[2], Catalina Curceanu[2], Luca de Paolis[2,6], Raffaele Del Grande[2,7], Laura Fabbietti[7,8], Carlo Guaraldo[2], Mihai Iliescu[2], Masahiko Iwasaki[9], Paolo Levi Sandri[2], Johann Marton[5], Marco Miliucci[2,6], Pawel Moskal[1], Kristian Piscicchia[2,10], Angels Ramos[11], Alessandro Scordo[2], Michał Silarski[1], Diana Laura Sirghi[2,4], Florin Sirghi[2,4], Antonio Spallone[2], Oton Vazquez Doce[7,8], Sławomir Wycech[12], Johann Zmeskal[5]

[1] *Department of Experimental Particle Physics and Applications, Jagiellonian University, ul. Łojasiewicza 11, 30-348 Cracow, Poland*
[2] *INFN, Laboratori Nazionali di Frascati, Via Enrico Fermi 54, 00044 Frascati RM, Italy*
[3] *Horia Hulubei National Institute of Physics and Nuclear Engineering, Str. Reactorului 30, P.O. BOX MG-6, Bucharest - Magurele, Romania*
[4] *Department of Physics, Faculty of Science, University of Zagreb, Horvatovac 102a, HR-10000 Zagreb, Croatia*
[5] *Stefan-Meyer-Institut für subatomare Physik, Kegelgasse 27, 1030 Vienna, Austria*
[6] *Università degli Studi di Roma Tor Vergata, Via Cracovia snc, 00133 Rome, Italy*
[7] *Physik Department E12, Technische Universität München, James-Franck-Str. 1, 85748 Garching, Germany*
[8] *Excellence Cluster "Origin and Structure of the Universe", Boltzmann str. 2, D-85748 Garching, Germany*
[9] *RIKEN, The Institute of Physics and Chemical Research, 2-1 Hirosawa, Wako, 351-0198 Saitama, Japan*
[10] *Museo Storico della Fisica e Centro Studi e Ricerche Enrico Fermi, Via Panisperna 89a, 00184 Rome, Italy*
[11] *Departament de Fisica Quantica i Astrofisica and Institut de Ciencies del Cosmos, Universitat de Barcelona, Marti i Franques 1, Martí i Franquès 1, 08028 Barcelona, Spain*
[12] *Department of Theoretical Physics, National Centre for Nuclear Research, ul. Pasteura 7, 02-093 Warsaw, Poland*

Received Day Month Year
Revised Day Month Year

The aim of the AMADEUS collaboration is to provide new experimental constraints to the antikaon-nucleon ($\bar{K}N$) strong interaction in the regime of non-perturbative QCD, investigating the low-energy K^- hadronic interactions with light nuclei like H, ^{4}He, ^{9}Be and ^{12}C. The unique low-momentum kaon beam produced at the DAΦNE collider is ideal to study K^- nuclear captures, both at-rest and in-flight. The large acceptance KLOE detector used as an active target allows to achieve excellent position and momentum resolutions. In this work a brief description of recent AMADEUS results is presented.

Keywords: strangeness, antikaon interactions in nuclear matter

PACS numbers:

1. Introduction

The AMADEUS (Anti-kaonic Matter At DAΦNE: An Experiment with Unraveling Spectroscopy) Collaboration[1–4] investigates the low-energy K^- induced reactions in light nuclear targets (the KLOE detector[5] material) in order to provide experimental constraints to the non-perturbative QCD in the strangeness sector, by exploiting the low momentum ($p_K \sim 127$ MeV/c), almost monochromatic, charged kaons produced in the decay of Φ mesons at-rest at the DAΦNE accelerator.[6]

The low-energy QCD studies in the strangeness sector face difficulties within the chiral perturbation theory (χPT), due to the appearance of the broad $\Lambda(1405)$ and $\Sigma(1385)$ resonances just below the $\bar{K}N$ threshold. To deal with this problem, chiral unitary models[7–13] and phenomenological potential models[14–19] were developed, leading however to contrasting predictions for the $\Lambda(1405)$ parameters and related kaonic nuclear bound states.

The $\Lambda(1405)$ resonance has a spin 1/2, isospin $I = 0$, strangeness S = -1 and negative parity and decays into $(\Sigma\pi)^0$ through the strong interaction. Although in Particle Data Group (PDG)[20] $\Lambda(1405)$ is listed as a four-stars resonance, its nature still remains an open issue. Experiments result in observation of different masses and widths of this resonance, depending on the production channel as well as the observed decay mode.[21] The position of the $\Lambda(1405)$ reflects the strength of the $\bar{K}N$ interaction, thus influencing the possible formation of K^- multi-nucleon bound states (it is predicted that in the $\bar{K}N$ subthreshold region kaon-nucleon interaction is attractive enough to form a bound state in the isospin I=0 channel[22,23]). According to the phenomenological models,[14–19] $\Lambda(1405)$ is interpreted as a pure strongly attractive $\bar{K}N$ bound state, which implies the prediction of K^- deeply bound in nuclear system. In the chiral models,[7–13] the $\Lambda(1405)$ resonance emerges as a superposition of two states (a high-mass state located around 1420 MeV, coupled to the $\bar{K}N$ production channel and a low-mass state at 1380 MeV, coupled to the $\Sigma\pi$ channel), resulting in much less attractive K^-N interaction, which leads to the prediction of slightly bound kaonic nuclear states.

A strong experimental effort was devoted to the search for a K^-pp state using two main approaches: proton-proton and heavy-ion collisions (DISTO[24] and HADES[25] experiments) and in-flight or stopped K^- interactions in light nuclei (FINUDA,[26] KEK-PS E549[27] and J-PARC E15[28,29] experiments). The binding energies (B.E.) and the widths (Γ) of the lightest kaonic-nuclear cluster, K^-pp, determined from experimental data are broadly spread and same of them in contrast to the calculated values based on chiral and phenomenological approaches. This is related to the fact that the extraction of the bound state signal in K^- absorption experiments is strongly affected by the yield and the shape of the competing K^- multi-nucleon absorption processes.[26,27] The first clear signal of the K^-pp kaonic nuclear bound state has been recently observed and investigated at J-PARC in the ^{3}He(K^-,Λp)n reaction.[29]

The activities of the AMADEUS collaboration are devoted to perform experimental investigations of the low-energy charged kaon-nucleon/nuclei interaction, ranging from the measurement of $\Lambda(1405)$ resonance properties to the clarification of the existence of the kaonic bound states.

This article reports on the studies of K^- single-nucleon absorption in ^{4}He leading to the determination for the first time of the non-resonant contribution in $\mathrm{K}^-\mathrm{N} \rightarrow \mathrm{Y}\pi$ reaction[30] below the $\bar{\mathrm{K}}\mathrm{N}$ threshold which is essential for studies of the $\Lambda(1405)$ resonance properties. Moreover, we present the investigation of the K^- interactions in ^{12}C nuclei resulting in the first complete characterization of the K^- two-, three- and four-nucleon absorptions (2NA, 3NA and 4NA) in the Λp and Σ^0p final states considering the possible existence of the K^-pp bound state.[31,32]

The article is divided into five sections. The features of the DAΦNE accelerator and the KLOE detector are introduced in Sec. 2, while in Sec. 3 and 4 the data analysis and the obtained results are discussed. The summary is presented in Sec. 5.

2. The experimental setup

The data sample investigated by the AMADEUS collaboration has been collected with the KLOE detection system[5] installed at the double ring e^+e^- DAΦNE collider[6] (as it is shown in the left panel in Fig. 1) designed to work at the center of mass energy of the ϕ particle.

DAΦNE (Double Annular Φ-factory for Nice Experiments) facility delivers a monochromatic, low momentum ($\sim$127 MeV/c) charged kaon beam from the ϕ-meson decays (BR($\mathrm{K}^+\mathrm{K}^-$) = (48.9±0.5)%) excellent to investigate the low-energy K^- - nucleus absorption processes. The back-to-back topology of the kaons pair production is extremely useful for the extrapolation of non-identified kaon tracks.

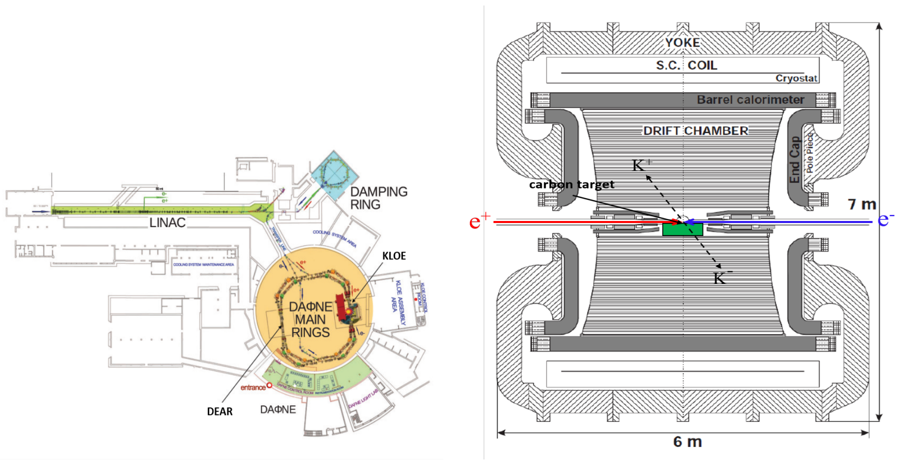

Fig. 1. Schematic view of the DAΦNE facility with the KLOE detector in one of the interaction points (left). The cross section of the KLOE detector with marked e^+e^- collision and $\phi \rightarrow K^+K^-$ decay (right).

The KLOE (KLOng Experiment) detector, characterized by a 4π geometry, is centered around the DAΦNE interaction region. The detector consists of a large Drift Chamber (DC)[33] of cylindrical shape and a calorimeter of fine sampling lead-scintillating fibers.[34] All components are immersed in an axial magnetic field of 0.52 T, provided by a superconducting solenoid. The KLOE detector cross section is presented in the right panel in Fig. 1.

The DC is filled with a mixture of Helium and Isobutane C_4H_{10} (90% of Helium and 10% of Isobutane in volume) and its inner radius, outer radius and length are equal to 0.25 m, 2 m and 3.3 m, respectively. The DC entrance wall is formed of 750 μm layer of Carbon fiber and 150 μm layer of Aluminum. The particle tracks reconstruction is performed with excellent position resolution, of $\sigma_{\rho\phi} \sim 200\mu$m in the transverse ρ - ϕ plane and of $\sigma_z \sim$ 2mm along the z-axis. The transverse momentum resolution for low-momentum tracks ($p <$ 300 MeV/c) is $\frac{\sigma_{p_T}}{p_T} \sim 0.4$.

The calorimeter is composed of a cylindrical barrel and two end-caps. Its volume ratio (lead/fibers/glue=42:48:10) is optimised for a high light yield and a high efficiency for photons in the range 20-300 MeV/c. The cluster position resolution along the fibers is $\sigma_{\parallel} = \frac{1.4cm}{\sqrt{(E/1GeV)}}$ while in the orthogonal direction is $\sigma_{\perp}$=1.4cm. The energy and time resolutions for photon clusters are given by $\frac{\sigma_E}{E_\gamma} = \frac{0.057}{\sqrt{(E_\gamma/1GeV)}}$ and $\sigma_t = \frac{57ps}{\sqrt{(E_\gamma/1GeV)}} \oplus$ 100 ps.

The analyses described below refer to a sample of 1.74 fb^{-1} integrated luminosity collected by the KLOE collaboration[5] during the 2004/2005 data campaign and to the data collected in summer 2012 for a high purity carbon target (graphite) installed inside the KLOE detector, between the beam pipe and the DC inner wall.

3. Resonant and non-resonant $Y\pi$ transition amplitudes below the $\bar{\text{K}}$N threshold

The experimental investigation of the $\Lambda(1405)$ resonance properties is challenging since the resonance line-shape is found to depend on both, the production mechanism and the observed decay channel. In case of $\Lambda(1405)$ production in K$^-$ induced reactions in light nuclear targets, two biases have to be taken into account. The first bias is the $\Sigma\pi$ invariant mass threshold imposed by the absorbing nucleon binding energy, which for K$^-$ capture at-rest on ^{4}He is about 1412 MeV, while for ^{12}C it is about 1416 MeV. The access to the $\bar{\text{K}}$N sub-threshold region corresponding to the $\Lambda(1405)$ high-mass predicted pole (about 1420 MeV) is possible via K$^-$N absorption in-flight. For a mean kaon momentum of 100 MeV/c, the $\Sigma\pi$ invariant mass threshold is shifted upwards by about 10 MeV.

Among the three $(\Sigma\pi)^0$ charge combinations $\Sigma^0\pi^0$ represents the so called "golden decay channel" being the best signature for the $\Lambda(1405)$ resonance free from the isospin I=0 background. The $\Sigma^0\pi^0$ invariant mass spectrum from K$^-$ captures in ^{12}C nuclei for two data samples[35] is presented in Fig. 2.

The black distribution corresponds to the 2004/2005 AMADEUS data campaign,

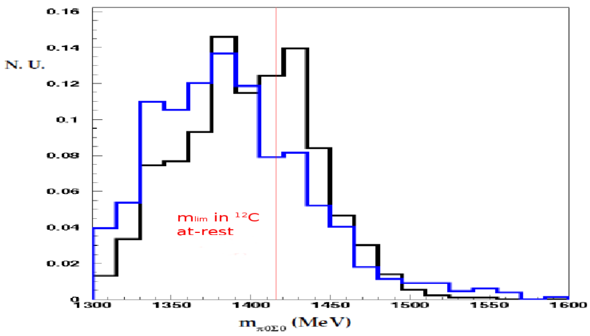

Fig. 2. The $m_{\Sigma^0\pi^0}$ invariant mass distribution from K$^-$ captures in the KLOE DC wall (black curve) and pure carbon graphite target (blue curve).

which includes both K$^-$ captures at-rest and in-flight, while the blue distribution, obtained from 2012 data, contains mainly K$^-$ captures at-rest. The blue and the black distributions are normalized to unity. A red line indicates the energy threshold corresponding to K$^-$ absorption in ^{12}C at-rest. A rich sample of in-flight K^{-12}C captures can be easily identified above the red line.

The second bias refers to the non-resonant K$^-$N $\rightarrow \Sigma\pi$ contribution that has to be subtracted in order to extract the $\Lambda(1405)$ shape. It was by us experimentally investigated for the first time in the K$^-$n $\rightarrow \Lambda\pi^-$ process, considering K$^-$n single nucleon absorptions in ^{4}He.[30] The measured $\Lambda\pi^-$ invariant mass, momentum and angular distributions were simultaneously fitted by means of dedicated Monte Carlo simulations based on the phenomenological K$^-$-nucleus absorption model developed in Ref.[36] In the performed fit, shown in Fig. 3, all the contributing reactions were taken into account, namely, non-resonant processes, resonant processes, the primary production of a Σ followed by the ΣN $\rightarrow \Lambda$N' conversion process and the contamination of K^{-12}C.

The analysis allowed to determine the non-resonant transition amplitude modulus which was found to be $|A_{K^-n\rightarrow\Lambda\pi^-}| = (0.334 \pm 0.018$ stat. $^{+0.034}_{-0.058}$ syst.) fm at (33$\pm$6) MeV below the $\bar{\mathrm{K}}$N threshold. The result (with combined statistical and systematic errors) is shown in Fig. 4 and compared with the theoretical predictions (Prague (P),[37] Kyoto-Munich (KM),[38] Murcia (M1,M2),[39] Bonn (B2,B4)[40]) rescaled for the K$^-$n $\rightarrow \Sigma\pi$ transition probabilities. This measurement can be used to test and constrain the *s*-wave K$^-$n $\rightarrow \Lambda\pi^-$ transition amplitude calculations.

4. K$^-$ multi-nucleon absorption cross sections and branching ratios in Λp and Σ^0p final states

The possible existence of the K$^-$pp bound state can be investigated in the low-energy K$^-$ induced reactions by reconstructing the proper decay channels. Recently, $\Lambda(\Sigma^0)$p decay modes were investigated by the AMADEUS collaboration in

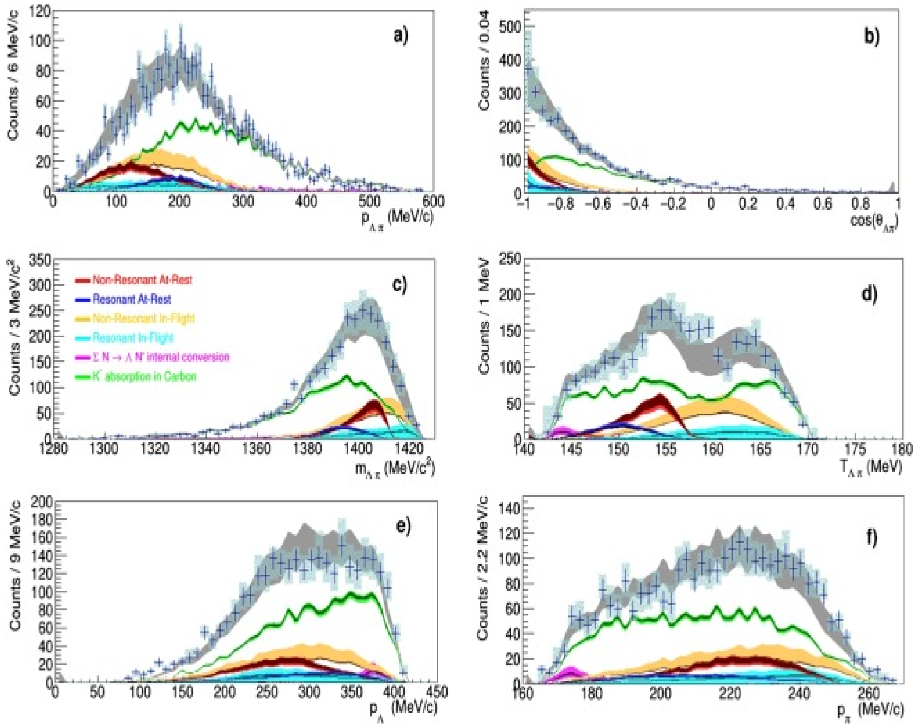

Fig. 3. Panels a-f: $p_{\Lambda\pi}$, $\cos(\theta_{\Lambda\pi})$, $m_{\Lambda\pi}$, $T_{\Lambda\pi}$, p_Λ and p_π distributions.[30] The experimental data and the corresponding statistical errors are represented by the black crosses, the systematic errors are light blue boxes. The different contributions included in the fit are shown by the colored histograms: non-resonant at-rest (red), resonant at-rest (blue), non-resonant in-flight (brown), resonant in-flight (cyan), ΣN $\to$ ΛN' internal conversion (magenta), K$^-$ absorptions in Carbon (green). The light and dark bands correspond to systematic and statistical errors, respectively. The gray band shows the total fit with the corresponding statistical error. The plot was adapted from Ref.[30]

K^{-12}C absorption.[31,32] These studies resulted in the first complete characterization of the K$^-$ two-, three- and four-nucleon absorptions (2NA, 3NA and 4NA).[32] The 2NA, 3NA and 4NA absorption branching ratios (BRs) and cross sections for low-momentum kaons in Λp and Σ^0p channels were determined by performing a simultaneous fit of the Λp invariant mass, Λp angular correlation, Λ and proton momenta with the simulated distributions for both direct Λ and Σ^0 productions followed by $\Sigma^0 \to \Lambda\gamma$ decay. The simulations were carried out taking into account calculations of K$^-$ nuclear capture at-rest and in-flight described in Refs.[36,42] The fitted spectra are shown in Fig. 5, while obtained BRs and cross sections are summarized in Table 1.

The BR of the Σ^0p direct production in K$^-$ 2NA quasi free interaction is found to be greater than the corresponding Λp production (R $= \frac{\mathrm{BR(K^-(pp)\to\Lambda p)}}{\mathrm{BR(K^-(pp)\to\Sigma^0 p)}} =$ $0.7 \pm 0.2(stat.)^{+0.2}_{-0.3}(syst.)$) which is in contrast to the pure phase spaces compar-

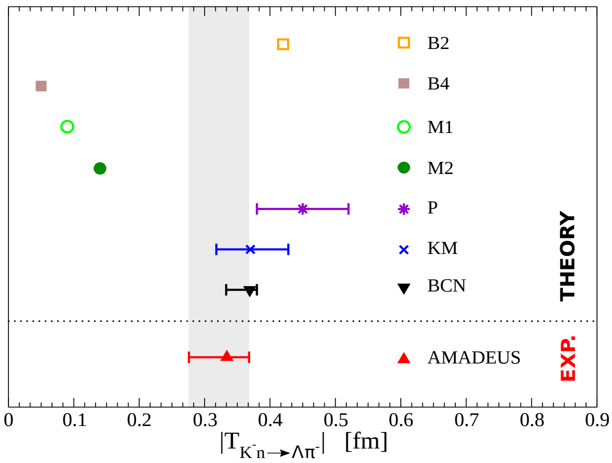

Fig. 4. Modulus of the measured non resonant $K^-n \rightarrow \Lambda\pi^-$ transition amplitude compared with theoretical calculations, see details in the text. Figure is adapted from Ref.[41]

ison ($R' = 1.22$). This evidences the dynamical effects involved in the measured processes and thus gives important information on the K^-N dynamics below the threshold.

The possible contribution of K^-pp bound system in Λp spectra was also investigated. It was found that K^-pp completely overlaps with the K^- 2NA-QF process, therefore it is impossible to extract the corresponding yield. In the further step, in order to compare the spectra with the corresponding FINUDA measurement, back-to-back Λp events were selected ($\cos\theta_{\Lambda p} <$ -0.8). As in the previous case, the obtained spectra can be completely described in terms of K^- multi-NA processes. The determined BRs are in agreement with those obtained from the fit presented in Fig. 5.

5. Summary

We presented in this work the AMADEUS investigations of the low energy interaction between K^- and nucleons/nuclei in light nuclear targets providing input for a better understanding of the non-perturbative quantum chromodynamics QCD in the strangeness sector. Studies of the K^-n single nucleon absorption in ^{4}He allowed to characterize for the first time the non-resonant $K^-N \rightarrow Y\pi$ production below the $\bar{K}N$ threshold which is crucial for the investigation of the $\Lambda(1405)$ characteristics. Studies of low-energy K^- captures on a solid carbon target result in a complete characterisation of the two-, three- and four-nucleon absorptions in the Λp and $\Sigma^0 p$ final states (BRs and cross sections). Moreover, it was found that the contribution from a possible K^-pp bound state completely overlaps with the K^- 2NA-QF process.

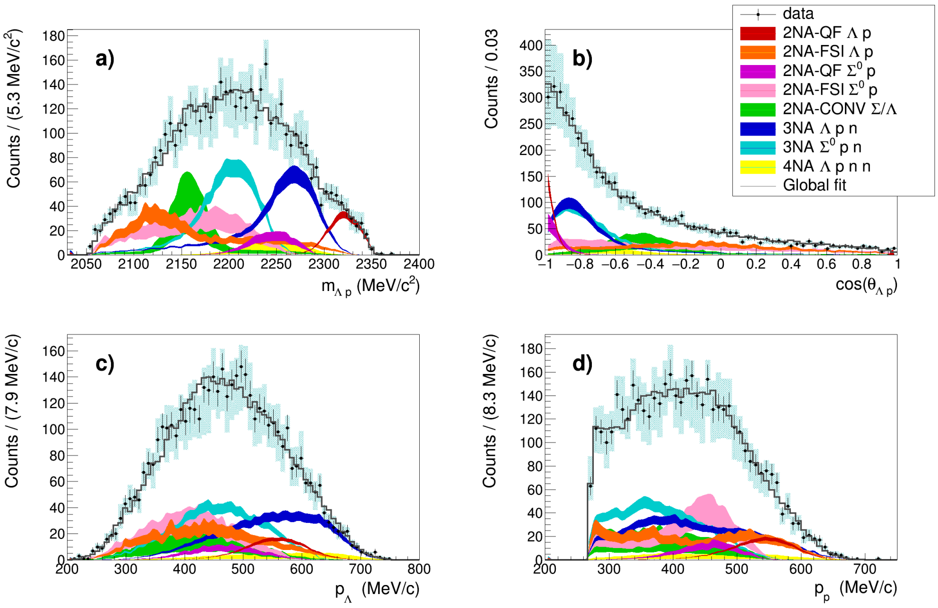

Fig. 5. Panels a-f: $m_{\Lambda p}$ (Λp invariant mass), $\cos(\theta_{\Lambda p})$ (cosine of angle between Λ and proton), p_Λ (Λ momentum) and p_p (proton momentum) distributions[32] for the K$^-$ absorption on $^{-12}$C listed in the legend. Black points represent the data, black error bars correspond to the statistical errors, cyan error bars correspond to the systematic errors. The gray line distributions represent the global fitting functions, the coloured distributions represent the different contributing processes according to the colour code reported in the legend and the widths correspond to the statistical error.

Table 1. Branching ratios (for the K$^-$ absorbed at-rest) and cross sections (for the K$^-$ absorbed in-flight) of the K$^-$ multi-nucleon absorption processes. The K$^-$ momentum is evaluated in the centre of mass reference frame of the absorbing nucleons, thus it differs for the 2NA and 3NA processes. The statistical and systematic errors are also given. The Table is adapted from Ref.[32]

σ (mb)	@ p_K (MeV/c)			
2NA-QF Λp	0.25 ± 0.02 (stat.) $^{+0.01}_{-0.02}$(syst.)	2.8 ± 0.3 (stat.) $^{+0.1}_{-0.2}$ (syst.)	@	128 ± 29
2NA-FSI Λp	6.2 ± 1.4(stat.) $^{+0.5}_{-0.6}$(syst.)	69 ± 15 (stat.) ± 6 (syst.)	@	128 ± 29
2NA-QF Σ^0p	0.35 ± 0.09(stat.) $^{+0.13}_{-0.06}$(syst.)	3.9 ± 1.0 (stat.) $^{+1.4}_{-0.7}$ (syst.)	@	128 ± 29
2NA-FSI Σ^0p	7.2 ± 2.2(stat.) $^{+4.2}_{-5.4}$(syst.)	80 ± 25 (stat.) $^{+46}_{-60}$ (syst.)	@	128 ± 29
2NA-CONV Σ /Λ	2.1 ± 1.2(stat.) $^{+0.9}_{-0.5}$(syst.)	-		
3NA Λpn	1.4 ± 0.2(stat.) $^{+0.1}_{-0.2}$(syst.)	15 ± 2 (stat.) ± 2 (syst.)	@	117 ± 23
3NA Σ^0pn	3.7 ± 0.4(stat.) $^{+0.2}_{-0.4}$(syst.)	41 ± 4 (stat.) $^{+2}_{-5}$ (syst.)	@	117 ± 23
4NA Λpnn	0.13 ± 0.09(stat.) $^{+0.08}_{-0.07}$(syst.)	-		
Global $\Lambda(\Sigma^0)$p	21 ± 3(stat.) $^{+5}_{-6}$(syst.)	-		

Acknowledgements

We acknowledge the KLOE/KLOE-2 Collaboration for their support and for having provided us the data and the tools to perform the analysis presented in this paper.

We acknowledge the CENTRO FERMI - Museo Storico della Fisica e Centro Studi e Ricerche "Enrico Fermi", for the project PAMQ. Part of this work was supported by the Austrian Science Fund (FWF): [P24756-N20]; Austrian Federal Ministry of Science and Research BMBWK 650962/0001 VI/2/2009; the Croatian Science Foundation, under project 8570; Polish National Science Center through grant No. UMO-2016/21/D/ST2/01155; EU Horizon 2020 STRONG-2020-No. 824093 project.

References

1. R. Del Grande, et al., *J. Phys.: Conf. Ser.* **1643** (2020) 012081.
2. M. Skurzok, et al., *Springer Proc. Phys.* **238** (2020) 937.
3. M. Skurzok, et al., *JPS Conf. Proc.* **26** (2019) 023011.
4. C. Curceanu, et al., *Acta. Phys. Pol. B* **46** (2015) 203.
5. F. Bossi, et al., *Riv. Nuovo Cim.* **31** (2008) 531.
6. A. Gallo, et al., *Conf. Proc. C* **060626** (2006) 604.
7. A. Dote, T. Hyodo, W. Weise, *Phys. Rev. C* **79** (2009) 014003.
8. A. Dote, T. Inoue, T. Myo, *Phys. Lett. B* **784** (2018) 405.
9. N. Barnea, A. Gal, E. Z. Liverts, *Phys. Lett. B* **712** (2012) 132.
10. Y. Ikeda, H. Kamano and T. Sato, *Prog. Theor. Phys.* **124** (2010) 533.
11. P. Bicudo, *Phys. Rev. D* **76** (2007) 031502.
12. M. Bayar and E. Oset, *Nucl. Phys. A* **914** (2013) 349.
13. T. Sekihara, E. Oset, A. Ramos, *PTEP* **2016** (2016) 12.
14. Y. Akaishi, T. Yamazaki, *Phys. Rev. C* **65** (2002) 044005.
15. Y. Ikeda and T. Sato, *Phys. Rev. C* **76** (2007) 035203.
16. S. Wycech, A. M. Green, *Phys. Rev. C* **79** (2009) 014001.
17. N. V. Shevchenko, A. Gal, J. Mares, *Phys. Rev. Lett.* **98** (2007) 082301.
18. J. Revai and N. V. Shevchenko, *Phys. Rev. C* **90** (2014) 034004.
19. S. Maeda, Y. Akaishi, T. Yamazaki, *Proc. Jpn. Acad. B* **89** (2013) 418.
20. P. A. Zyla et al. (Particle Data Group), *Prog. Theor. Exp. Phys.* **2020** 083C01 (2020).
21. T. Hyodo and D. Jido, *Prog. Part. Nucl. Phys.* **67** (2012) 55.
22. S. Wycech, *Nucl. Phys. A* **450** (1986) 399c.
23. Y. Akaishi, T. Yamazaki, *Phys. Lett. B* **535** (2002) 70.
24. M. Maggiora, et al., *Nucl. Phys. A* **835** (2010) 43.
25. G. Agakishiev, Phys. Lett. B 742 (2015) 242.
26. M. Agnello, et al., *Phys. Rew. Lett.* **94** (2005) 212303.
27. T. Suzuki, et al., *Mod. Phys. Lett. A* **23** (2008) 2520.
28. Y. Sada, et al. *PTEP 2016* **(5)** (2016) 051D01.
29. S. Ajimura, et al., *Phys. Lett. B* **789** (2019) 620.
30. K. Piscicchia, et al., *Phys. Lett. B* **782** (2018) 339.
31. O. Vazques Doce, et al., *Phys. Lett. B* **758** (2016) 134.
32. R. Del Grande, et al., *Eur. Phys. J. C* **79** (2019) 190.
33. M. Adinolfi, et al., [KLOE Collaboration], *Nucl. Inst. Meth. A* **488** (2002) 51.
34. M. Adinolfi, et al. [KLOE Collaboration], *Nucl. Inst. Meth. A* **482** (2002) 364.
35. K. Piscicchia, PhD thesis (2013), http://www.infn.it/thesis/thesis_dettaglio.php?tid=7097.
36. K. Piscicchia, S. Wycech and C. Curceanu, *Nucl. Phys. A* **954** (2016) 75.
37. A. Cieplý and J. Smejkal, *Nucl. Phys. A* **881** (2012) 115.
38. Y. Ikeda, T. Hyodo and W. Weise, *Nucl. Phys. A* **881** (2012) 98.
39. Z. H. Guo and J. A. Oller, *Phys. Rev. C* **87** (2013) 035202.
40. M. Mai and U. G. Meissner, *Eur. Phys. J. A* **51** (2015) 30.

41. A. Feijoo, V. K. Magas and A. Ramos, *AIP Conf. Proc.* **2130** no. 1 (2019) 040013.
42. R. Del Grande, K. Piscicchia, S. Wycech, Phys. Pol. B **48** (2017) 1881.